Atmospheric Environment xxx (2014) 1–8

Contents lists available at ScienceDirect

Atmospheric Environment

journal homepage: www.elsevier.com/locate/atmosenv

Causes of increasing ozone and decreasing carbon monoxide in springtime at the Mt. Bachelor Observatory from 2004 to 2013

L.E. Gratz [a, *], D.A. Jaffe [a, b], J.R. Hee [a]

[a] School of Science and Technology, University of Washington-Bothell, 18115 Campus Way NE, Bothell, WA 98011, USA
[b] Department of Atmospheric Sciences, University of Washington, 408 Atmospheric Sciences-Geophysics Building, Seattle, WA 98195, USA

HIGHLIGHTS

- We examined 10-year trends in springtime O_3 and CO at the Mt. Bachelor Observatory.
- Median O_3 increased by 1.7% yr^{-1} while median CO decreased by -1.9 yr^{-1}.
- HYSPLIT cluster analysis suggests the impact of ALRT on western U.S. springtime O_3.
- Reductions in Northern Hemisphere emissions likely influenced springtime CO.
- Trends suggest that North Pacific OH may have increased over the study period.

ARTICLE INFO

Article history:
Received 18 February 2014
Received in revised form
9 May 2014
Accepted 30 May 2014
Available online xxx

Keywords:
Ozone
Carbon monoxide
Western U.S.
Long-term trends
Trajectory cluster analysis
Asian long-range transport

ABSTRACT

We report trends in springtime ozone (O_3) and carbon monoxide (CO) at the Mt. Bachelor Observatory (MBO) in central Oregon, U.S.A. from 2004 to 2013. Over the 10-year period the median and 95th percentile springtime O_3 increased by 0.76 ± 0.61 ppbv yr^{-1} (1.7 ± 1.4% yr^{-1}) and 0.87 ± 0.73 ppbv yr^{-1} (1.5 ± 1.2% yr^{-1}), respectively. These trends are consistent with reported positive trends in springtime O_3 in the western U.S. In contrast, median CO decreased by -3.1 ± 2.4 ppbv yr^{-1} (-1.9 ± 1.4% yr^{-1}), which is highly similar to springtime North Pacific surface flask measurements from 2004 to 2012. While a 10-year record is relatively short to evaluate long-term variability, we incorporate transport model analysis and contextualize our measurements with reported northern mid-latitude trends over similar time frames to investigate the causes of increasing O_3 and decreasing CO at MBO. We performed cluster analysis of 10-day HYSPLIT back-trajectories from MBO and examined O_3 and CO trends within each cluster. Significant positive O_3 trends were associated with high-altitude, rapid transport from East Asia. Significant negative CO trends were most associated with transport from the North Pacific and Siberia, as well as from East Asia. The rise in springtime O_3 is likely associated with increasing O_3 precursor emissions in Asia and long-range transport to the western U.S. The decline in springtime CO appears linked to decreasing Northern Hemisphere background CO, largely due to anthropogenic emissions reductions in Europe and North America, and also to a recently reported decline in total CO output from China caused by more efficient combustion. These springtime O_3 and CO trends suggest that hydroxyl radical (OH) mixing ratios in the North Pacific may have increased over the study period.

1. Introduction

Surface ozone (O_3) is integral to tropospheric chemistry and has adverse impacts on human health and the environment (Monks et al., 2009; McDonald-Buller et al., 2011). It is a secondary pollutant produced through photochemical reactions involving naturally or anthropogenically emitted nitrogen oxides (NO_x), carbon monoxide (CO), methane (CH_4), and volatile organic compounds (VOCs) (Monks et al., 2009; Cooper and Ziemke, 2013). It is destroyed by reactions involving water vapor and photolysis and is the major source of the hydroxyl radical (OH) (Monks et al., 2009; Parrish et al., 2013). Ozone also originates in the stratosphere and can be transported to the troposphere (Langford et al., 2009; Lin et al., 2012a). The O_3 lifetime is days in the boundary layer, but weeks in the free troposphere; thus it can be transported on continental scales (Zhang et al., 2008).

* Corresponding author.
E-mail address: lgratz@uw.edu (L.E. Gratz).

http://dx.doi.org/10.1016/j.atmosenv.2014.05.076
1352-2310/

Tropospheric O_3 in northern mid-latitudes has a well-known seasonal cycle linked to photochemistry, with a summer maximum in urban areas and late spring maximum in remote areas (Parrish et al., 2013). In some locations, elevated springtime O_3 has also been attributed to stratosphere-to-troposphere transport (Langford et al., 2009). Peak O_3 concentrations have recently shifted to earlier in the year, perhaps due to changes in atmospheric transport, emissions, and/or climate change (Parrish et al., 2013). Lin et al. (2014) reported that seasonal O_3 trends in the sub-tropical North Pacific are influenced by a combination of precursor emissions and decadal-scale shifts in atmospheric circulation, demonstrating how climate variability may impact surface O_3.

Recent changes in O_3 precursor emissions have had a demonstrated impact on regional O_3 production (Cooper and Ziemke, 2013; Hartmann et al., 2013). For example, surface O_3 increased at some northern mid-latitude European locations from 1950 until the late 1990s, likely due to economic and industrial growth; however, the rate of O_3 production at those sites has since slowed or declined, whereas surface O_3 has increased in East Asia since 1990 while downwind of Asia O_3 trends are variable (Parrish et al., 2012; Cooper and Ziemke, 2013; Hartmann et al., 2013; Oltmans et al., 2013). In the U.S., NO_x emissions controls have led to significant reductions in summertime O_3 and in the frequency and magnitude of high-O_3 events at several eastern U.S. sites (Cooper et al., 2012; He et al., 2013; Rieder et al., 2013). In contrast, springtime O_3 has increased significantly in the western U.S. free troposphere and at 50% of rural surface sites, likely due to trans-Pacific transport of Asian air masses that can increase baseline free tropospheric O_3 (Cooper et al., 2012). High-O_3 events at high-elevation western U.S. sites have been linked to Asian long-range transport (ALRT) and subsidence of O_3-rich air from the upper troposphere/lower stratosphere (UT/LS) (Ambrose et al., 2011; Lin et al., 2012a, 2012b). The U.S. primary O_3 National Ambient Air Quality Standards (NAAQS) is 75 ppbv, but reduction to 60–70 ppbv has been proposed (U.S. EPA, 2010). In the western U.S., where free tropospheric air affected by inter-continental pollution transport or episodic stratospheric intrusions can significantly influence surface O_3, NAAQS compliance may be a challenge (Parrish et al., 2010; Jaffe, 2011; Lin et al., 2012a, 2012b; Wigder et al., 2013a).

Carbon monoxide (CO) is emitted to the atmosphere as a product of incomplete combustion (e.g. fossil fuel and biomass burning) and is a precursor for carbon dioxide (CO_2) and O_3, while reaction with OH is the dominant sink (Worden et al., 2013). The CO lifetime is weeks to months; thus it has been used as a tracer of long-range pollution transport to the western U.S. (Price et al., 2004; Weiss-Penzias et al., 2006). Over the past decade or more, anthropogenic CO emissions in Europe and North America have declined, while emissions from China and India have increased; however, anthropogenic emissions inventories show large discrepancies, while biomass burning emissions estimates vary both spatially and temporally (Granier et al., 2011; Tohjima et al., 2013). Yet recent declines in Northern Hemisphere CO (Novelli et al., 2003; Hartmann et al., 2013; Worden et al., 2013) may suggest the impact of regional anthropogenic emissions reductions on atmospheric CO.

Here, we present springtime O_3 and CO trends from 2004 to 2013 at the Mt. Bachelor Observatory (MBO) in central Oregon, U.S.A. The location and elevation of MBO (43.979°N, 121.687°W, 2763 m asl) and the lack of large local anthropogenic emission sources upwind are optimal for sampling free tropospheric air and ALRT (Weiss-Penzias et al., 2006; Ambrose et al., 2011; Fischer et al., 2011). The greatest influence of trans-Pacific transport on the western U.S. is observed in spring due to ventilation of the East Asian boundary layer by mid-latitude cyclones and convection, and circulation of trans-Pacific pollution plumes around the Pacific High (Liang et al., 2004; Stohl et al., 2002; Zhang et al., 2008). We acknowledge that a 10-year record is relatively short for trend analysis; however, free troposphere measurements, including ozonesonde and aircraft measurements, have varying limitations related to data frequency and sampling location, and yet these datasets all provide important insights into global trends. While the MBO observations do not allow for examining inter-decadal variability in tropospheric concentrations and atmospheric transport, we combine measurements with transport model analysis and other reported long-term trends to identify possible causes of springtime O_3 and CO trends at this western U.S. free tropospheric site over the 10-year study period.

2. Methods

2.1. Measurements at MBO

Measurements at MBO began in February 2004. Continuous measurements include a suite of chemical (e.g. O_3, CO, aerosol scattering, mercury) and meteorological (e.g. wind speed/direction, temperature, relative humidity) parameters (Ambrose et al., 2011). Non-continuous measurements (e.g. for specific seasons or studies) include compounds such as nitrogen oxides (NO_x and NO_y) and peroxy acetyl nitrate (PAN).

Ozone measurements are made using a Dasibi 1008 RS UV Photometric Ozone Analyzer (Weiss-Penzias et al., 2006; Ambrose et al., 2011). Monthly automated zeroes are performed using a charcoal scrubber cartridge. The analyzer is calibrated every six months with an O_3 generator referenced to a Washington State Department of Ecology transfer standard, which is calibrated against the EPA Region 9 Standard Reference Photometer. The method detection limit (MDL) is 1 ppbv and the estimated total uncertainty is ±2% (Ambrose et al., 2011).

Carbon monoxide was measured during spring 2004 using a Thermo Electron Corporation (TECO) 48C nondispersive infrared analyzer, and thereafter using a TECO 48C Trace Level Enhanced (TLE) analyzer (Ambrose et al., 2011) through April 2012. These analyzers were calibrated every 24 h with a ±2% NIST-traceable working standard of 400–500 ppb referenced to a NOAA-certified breathing air primary standard. Zeroes were performed every two hours. The MDL was 20 ppbv and the estimated total uncertainty in hourly-averaged mixing ratios was ±6%. Since 1-May-2012, CO has been measured using the Picarro G2302 Cavity Ring-Down Spectrometer (Chen et al., 2013). Calibrations are performed every eight hours using NOAA calibration gas standards, which are referenced to the World Meteorological Organization's (WMO) mole fraction calibration scale. The estimated MDL is 1 ppbv with estimated total uncertainty of ±3.4%.

Although CO was measured using different instruments over the study period, they were consistently calibrated using certified calibration gases. Additionally, the TECO 48C TLE and Picarro G2302 analyzers were operated concurrently with a NOAA Programmable Flask Package during 2012. The Picarro measurements compared extremely well against discrete flask measurements ($y = 0.97x + 2.4$; $r^2 = 0.97$; $n = 145$). A comparison of hourly-averaged TECO 48C TLE versus Picarro G2302 CO measurements demonstrated that the TECO was relatively noisier than the Picarro ($y = 1.06x - 13.7$; $r^2 = 0.99$; $n = 2959$). At the average springtime hourly CO mixing ratio from April 2004 to April 2012 (144 ppbv; typical of free tropospheric values), we calculated a mean bias of −5 ppbv for the TECO measurements. We applied the above equation to the TECO CO measurements from April 2004 through April 2012 to correct for this bias and used the corrected data in this manuscript. Springtime CO trends were highly similar between corrected and uncorrected data. Additional information on the CO measurement inter-comparison and springtime trends calculated

Please cite this article in press as: Gratz, L.E., et al., Causes of increasing ozone and decreasing carbon monoxide in springtime at the Mt. Bachelor Observatory from 2004 to 2013, Atmospheric Environment (2014), http://dx.doi.org/10.1016/j.atmosenv.2014.05.076

using the uncorrected data are provided in the Supplemental Information.

Annually-averaged hourly data from 2004 through 2013 did not demonstrate significant trends in O_3 or CO; however, both species undergo strong seasonal variability that should be considered when determining long-term trends (Parrish et al., 2013; Strode and Pawson, 2013; Worden et al., 2013). Spring (1-April–31-May) was the only season with significant linear trends in O_3 and CO. When we included March the springtime trends were not statistically significant and March median mixing ratios did not display significant linear trends. Our election to focus on April–May is consistent with prior analyses of springtime long-range transport in the North Pacific (Forster et al., 2004; Weiss-Penzias et al., 2006; Zhang et al., 2008; Cooper et al., 2010; Fischer et al., 2011). We were unable to detect significant trends in CO in other seasons in part due to insufficient (<50%) data coverage in several months (Fig. SI-6). Ozone, CO and other parameters at MBO also vary greatly during summer and early fall due to wildland fire activity, a topic considered in other studies (Wigder et al., 2013b).

For our analyses we used hourly-averaged measurements from all hours of the day. We assume (following Parrish et al. 2012) that springtime regressions which are not filtered for baseline or boundary layer air provide accurate representations of long-term baseline trends at the high-elevation MBO site. This assumption is reasonable given the high percentage of hours/day that MBO is in the free troposphere (Ambrose et al., 2011) and the lack of local emission sources that influence springtime boundary layer air.

2.2. HYSPLIT back-trajectory cluster analysis

We computed 10-day air mass back-trajectories from MBO for every hour in April–May 2004–2013 using the Hybrid Single-Particle Lagrangian Integrated Trajectory (HYSPLIT) Model Version 4 (Draxler and Hess, 1998) with gridded meteorological data from the National Oceanographic and Atmospheric Administration's Air Resources Laboratory (NOAA-ARL). For 2004, we used National Center for Environmental Prediction (NCEP) 2.5° × 2.5° gridded meteorological data with a starting height of 1800 m above ground level (agl). For 2005–2013 we used Global Data Assimilation System (GDAS) 1° × 1° gridded meteorological data with a starting height of 1500 m agl. Starting heights were chosen based on the terrain height for the grid box containing MBO in each dataset (Ambrose et al., 2011; Fischer et al., 2011).

We applied the HYSPLIT Trajectory Cluster Analysis using trajectories starting every fourth hour beginning with 0:00 UTC (6 trajectories per day). HYSPLIT computes latitude/longitude endpoints every hour along each trajectory, and we used every 12th endpoint in the clustering procedure. HYSPLIT excluded four trajectories due to insufficient (<240 h) endpoint data. In total, 3655 trajectories were included and eight distinct clusters were identified. To merge the hourly observations with the every-fourth-hour trajectories, we averaged the hourly measurements within two hours before and after each trajectory start time.

2.3. Additional CO observations

We obtained monthly-averaged CO flask measurements for April–May 2004–2012 from the NOAA Earth System Research Laboratory (ESRL) Global Monitoring Division (GMD) carbon cycle surface flask sampling network (Novelli and Masarie, 2013). We selected three sites to represent the North Pacific region: Shemya, AK (SHM; 55.21N, 162.72W, 21 m asl), Sand Island, Midway (MID; 28.21N, 177.38W, 11 m asl), and Mauna Loa, HI (MLO; 19.54N, 155.58W, 3397 m asl).

We also obtained ascending mode total column CO and CO mixing ratios at 618 hPa from the Atmospheric Infrared Sounder (AIRS) onboard the Aqua satellite (airs.jpl.nasa.gov). We used monthly mean CO values for April–May 2004–2012 in the region surrounding MBO (42–45°N, 124–121°W) to compute springtime CO trends.

2.4. Statistical methods

We calculated trends by linear regression with a one-way ANOVA. We calculated annual percent changes by dividing the slope of the linear regression by the intercept. We report slopes with 95% confidence intervals and refer to trends as statistically significant for $p < 0.05$.

3. Results

3.1. Springtime O_3 and CO trends

From 2004 to 2013, median springtime O_3 increased significantly by 0.76 ± 0.61 ppbv yr^{-1} (1.7 ± 1.4% yr^{-1}; $r^2 = 0.51$, $p = 0.02$; Fig. 1). Mean O_3 similarly increased by 0.73 ± 0.54 ppbv yr^{-1} (1.6 ± 1.2% yr^{-1}, $r^2 = 0.54$, $p = 0.01$). The 95th percentile increased by 0.87 ± 0.73 ppbv yr^{-1} (1.5 ± 1.2% yr^{-1}; $r^2 = 0.49$, $p = 0.02$), while the 5th percentile did not have a significant linear trend (Fig. 1).

In contrast, median springtime CO significantly decreased from 2004 to 2013 by −3.1 ± 2.4 ppbv yr^{-1} (−1.9 ± 1.4% yr^{-1}, $r^2 = 0.54$, $p = 0.02$; Fig. 2). Mean CO also decreased by −3.2 ± 2.9 ppbv yr^{-1} (−1.9 ± 1.8% yr^{-1}, $r^2 = 0.44$, $p = 0.04$). The 5th and 95th percentiles showed decreasing tendencies but trends were not significant (Fig. 2).

3.2. HYSPLIT cluster analysis

3.2.1. Cluster characterization

Fig. 3 displays the mean back-trajectory path and altitude for each HYSPLIT cluster. These mean paths represent hundreds of trajectories in most cases (Table SI-1). The increasing uncertainty in each trajectory with distance from the starting location (Kahl and Samson, 1986) and the overall representativeness of back-trajectory clusters (Moody et al., 1998) have been established; thus, the mean paths actually represent a broad swath indicating the likely transport direction and altitude. These suggested pathways are, however, useful for categorizing the long-term transport regimes at MBO.

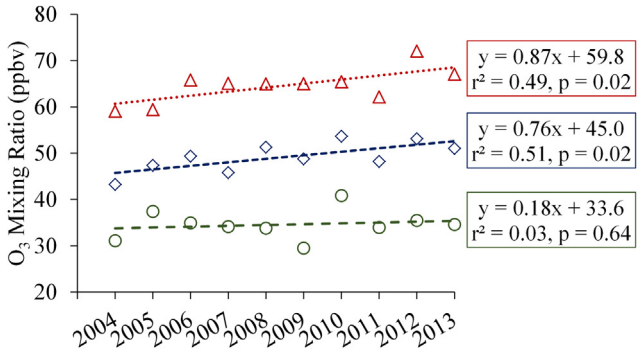

Fig. 1. 5th percentile (green circles), median (blue diamonds), and 95th percentile (red triangles) springtime O_3 mixing ratios at MBO from 2004 to 2013, with associated linear regressions. (For interpretation of the references to color in this figure legend, the reader is referred to the web version of this article.)

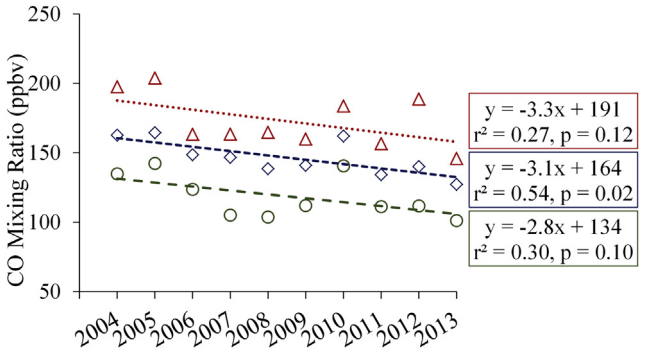

Fig. 2. 5th percentile (green circles), median (blue diamonds), and 95th percentile (red triangles) springtime CO mixing ratios at MBO from 2004 to 2013, with associated linear regressions. (For interpretation of the references to color in this figure legend, the reader is referred to the web version of this article.)

Clusters 2, 3, and 5 represent high-altitude trans-Pacific transport in the free troposphere from regions of East Asia, with Cluster 2 displaying the fastest long-range transport (Fig. 3). Clusters 1 and 6 represent transport from the North Pacific, with Cluster 6 depicting slower flow at a lower altitude. Clusters 1, 2, and 3 have the highest O_3 and CO mixing ratios (Table SI-1). The mean water vapor content in these three clusters is <3.28 g/kg (Table SI-1), which for MBO in spring suggests predominantly free tropospheric air (Ambrose et al., 2011). Clusters 4 and 7 represent relatively low-altitude flow over the Pacific, with mean WV contents >4 g/kg demonstrating a possible marine boundary layer influence (Table SI-1). Cluster 7 has the lowest mean, 5th and 95th percentile O_3 and CO (Table SI-1). Cluster 8 contains the fewest number of trajectories ($n = 83$) and is the most unique in its transport direction.

3.2.2. O_3 and CO trends within HYSPLIT clusters

Shifts in atmospheric circulation on inter-annual to decadal time scales can influence surface concentrations (Lin et al., 2014); however, when considering the number of trajectories assigned to each cluster from 2004 to 2013 we did not observe significant trends in the number of trajectories assigned to any cluster. Therefore, springtime O_3 and CO trends could not be attributed to more or less frequent transport from any of the identified source regions.

Tables 1 and 2 display the O_3 and CO trends within Clusters 1–7. Trends were not computed for Cluster 8 because no trajectories were assigned to it in 2004, 2007, or 2010. Clusters 2, 3, and 5 have significant positive trends in median O_3 of 0.91 ± 0.79, 1.0 ± 0.76, and 0.91 ± 0.69 ppbv yr^{-1}, respectively (1.8% yr^{-1} to 2.2% yr^{-1}). Cluster 3 also has a positive trend in the 5th percentile (1.0 ± 0.92 ppbv yr^{-1}), while Clusters 3, 4, and 5 have positive trends in the 95th percentile (0.93 ± 0.89, 1.9 ± 1.5, and 1.3 ± 1.2 ppbv yr^{-1}, respectively).

Springtime CO shows negative trends within every cluster, but not all are statistically significant (Table 2). Clusters 1, 3, 5, and 6 have significant declines in median CO of −5.4 ± 3.1 ppbv yr^{-1}, −3.9 ± 3.4 ppbv yr^{-1}, −2.8 ± 2.7 ppbv yr^{-1}, and −2.4 ± 2.2 ppbv yr^{-1}, respectively (−1.5% yr^{-1} to −2.9% yr^{-1}). Clusters 1 and 6 also have negative trends in the 5th percentile (−3.3 ± 3.1 ppbv yr^{-1} and −3.0 ± 2.1 ppbv yr^{-1}).

4. Discussion

A recent analysis estimated that 13 years of consistent observations would be needed to detect an O_3 trend at MBO with 95% confidence; however, that estimate assumed a 1% yr^{-1} O_3 increase (Fischer et al., 2011). Using 10 years of consistent springtime

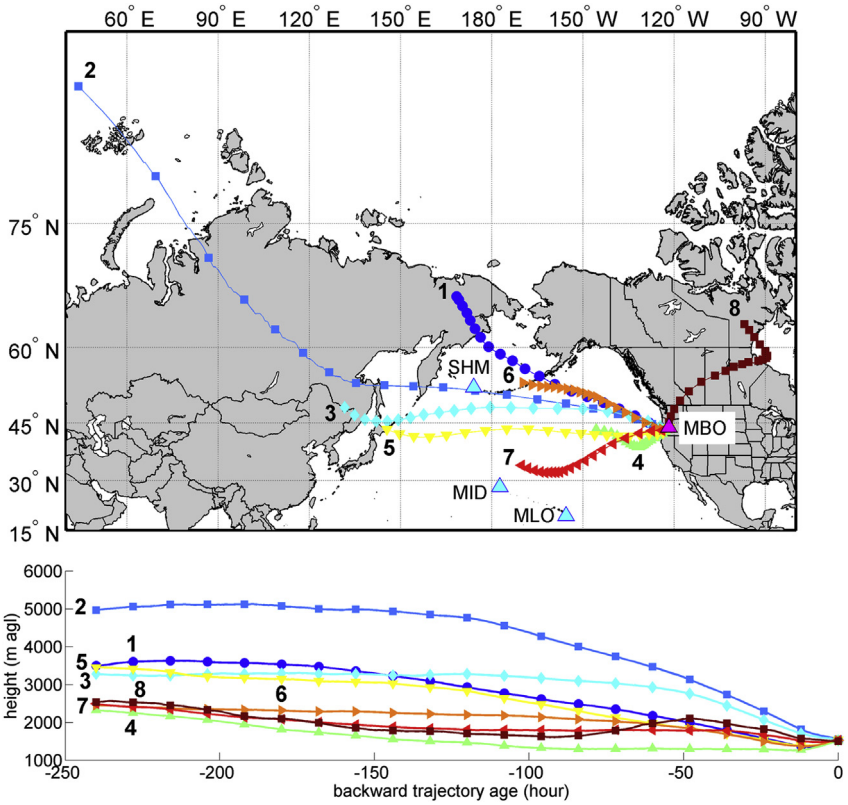

Fig. 3. Locations of the Mt. Bachelor Observatory (MBO; magenta triangle) and NOAA carbon cycle surface flask sites Shemya (SHM), Sand Island Midway (MID), and Mauna Loa (MLO) (light blue triangles), with mean air mass back-trajectories (map) and mean trajectory heights (m agl; lower panel) for each HYSPLIT cluster. (For interpretation of the references to color in this figure legend, the reader is referred to the web version of this article.)

Please cite this article in press as: Gratz, L.E., et al., Causes of increasing ozone and decreasing carbon monoxide in springtime at the Mt. Bachelor Observatory from 2004 to 2013, Atmospheric Environment (2014), http://dx.doi.org/10.1016/j.atmosenv.2014.05.076

Table 1
Linear regression statistics for springtime O_3 within HYSPLIT Clusters 1–7. Trends for Cluster 8 were not computed because no trajectories were assigned to it in 2004, 2007, or 2010. Bold values indicate $p < 0.05$.

O_3	Mean				Median				5th percentile				95th percentile			
Cluster #	m (ppbv/yr)	b (ppbv)	r^2	p	m (ppbv/yr)	b (ppbv)	r^2	p	m (ppbv/yr)	b (ppbv)	r^2	p	m (ppbv/yr)	b (ppbv)	r^2	p
1	0.36	48.8	0.10	0.37	0.39	47.5	0.15	0.28	−0.25	42.1	0.05	0.52	1.10	59.7	0.21	0.18
2	**0.84**	**50.2**	**0.44**	**0.04**	**0.91**	**49.1**	**0.47**	**0.03**	0.92	36.2	0.34	0.08	0.93	65.1	0.17	0.24
3	**0.93**	**47.9**	**0.70**	**0.00**	**1.02**	**47.2**	**0.54**	**0.02**	**1.00**	**32.8**	**0.44**	**0.04**	**0.93**	**62.7**	**0.42**	**0.04**
4	0.78	42.7	0.31	0.10	0.71	43.3	0.23	0.16	−0.01	32.0	0.00	0.99	**1.93**	**52.3**	**0.54**	**0.02**
5	**0.86**	**43.5**	**0.49**	**0.02**	**0.91**	**43.4**	**0.54**	**0.02**	0.02	32.1	0.00	0.98	**1.33**	**54.8**	**0.46**	**0.03**
6	0.59	45.2	0.27	0.13	0.52	45.4	0.19	0.20	0.68	32.5	0.23	0.16	0.90	56.6	0.32	0.09
7	0.53	41.2	0.14	0.29	0.79	40.2	0.24	0.15	−0.22	29.2	0.02	0.68	N/A	N/A	N/A	N/A

measurements, we observed a faster rate of increase in median springtime O_3 and a significant negative trend in median CO, both with 95% confidence. We examine these trends with respect to emissions estimates and other reported long-term trends to identify possible causes for increasing O_3 and decreasing CO at MBO.

4.1. O_3

The positive trend in median springtime O_3 at MBO is consistent with recent observations of increasing O_3 in the western U.S. reported by Cooper et al. (2010, 2012). They examined O_3 mixing ratios above western North America (3–8 km ASL) in April–May 1995–2008 and 1995–2011 and identified significant trends in median O_3 of 0.63 ± 0.34 ppbv yr^{-1} and 0.41 ± 0.27 ppbv yr^{-1}, respectively. The 95th percentile O_3 also increased from 1995 to 2011 (0.63 ± 0.66 ppbv yr^{-1}; $p = 0.06$) but was not significant ($p < 0.05$) (Cooper et al., 2010, 2012). The overall increase in springtime free tropospheric O_3 from 1995 to 2011 was 6.5 ppbv in the western U.S. (Cooper et al., 2012), whereas springtime O_3 at MBO increased by 7.6 ppbv from 2004 to 2013.

Ozone trends have also been reported at rural U.S. surface sites. From 1987 to 2004, deseasonalized monthly-mean O_3 increased at seven western U.S. sites by 0.19–0.51 ppbv yr^{-1} (Jaffe and Ray, 2007). From 1990 to 2010, 50% of western U.S. surface sites showed significant increases in median springtime (defined as March–April–May) O_3 while no site had a significant decrease, and 25% of sites had significant increases in the 95th percentile (Cooper et al., 2012). In contrast, 41% of eastern U.S. sites saw a decrease in 95th percentile springtime O_3, while in summer 66%, 20%, and 83%, of sites had significant decreases in the median, 5th percentile, and 95th percentile, respectively, suggesting the impact of U.S. emissions controls (Cooper et al., 2012).

Springtime trans-Pacific O_3 transport from Asia to North America is well-documented (Jaffe et al., 2003; Liang et al., 2004; Price et al., 2004; Zhang et al., 2008; Lin et al., 2012b), and increasing emissions of O_3 precursors in East Asia have been suggested as a possible explanation for rising springtime O_3 concentrations in the western U.S. (Cooper et al., 2010, 2012; Parrish et al., 2012). In China, anthropogenic NO_x emissions have approximately doubled in the past two decades (Granier et al., 2010; Mijling et al., 2013; Zhao et al., 2013). Although NO_x emissions in Japan and Korea have declined recently due to local environmental policies and economic downturns (Mijling et al., 2013), NO_x emissions from China contribute to tropospheric column NO_2 in these locations and have seemingly influenced an increase in springtime surface O_3 in South Korea (Lee et al., 2014). Similarly, while O_3 production in the eastern U.S. and in parts of Europe is generally decreasing (or the rate of increase is slowing) due to local anthropogenic NO_x emissions reductions, increasing East Asian NO_x emissions have likely resulted in an increase in western U.S. baseline O_3 (Cooper et al., 2010, 2012; Parrish et al., 2012).

Ozone mixing ratios at MBO, like other parts of the western U.S., can also be affected by the UT/LS. Using the GEOS-Chem model, Jaeglé et al. (2003) calculated that the UT/LS provides 28% of O_3 to the 0–6 km column over the Pacific. Lin et al. (2012a) calculated using the AMS3 model that 36% of surface O_3 at high elevation sites in the western US is from the UT/LS. Episodic transport events can also significantly enhance O_3 mixing ratios both at high-elevation sites like MBO in the western U.S. (Ambrose et al., 2011; Lin et al., 2012a) and at lower elevation sites (Lefohn et al., 2011). Changes in the 95th percentile O_3 (Fig. 1) may reflect variability in the frequency of these UT/LS episodes. Ambrose et al. (2011) examined free tropospheric high-O_3 events (8-h average > 70 ppbv) at MBO. Of 18 classifiable events identified between March–September 2004–2009, 44% were associated with downward mixing from the UT/LS, 22% with ALRT, and 33% with a combination of UT/LS and ALRT (Ambrose et al., 2011). Therefore, while UT/LS episodes influence springtime O_3 at MBO, they are likely too infrequent to drive the 10-year positive trend in springtime O_3. Cooper et al. (2010) also did not identify a trend in stratospheric intrusion frequency from 1995 to 2008 in the western U.S. free troposphere and isolating these episodes from long-term datasets did not change the overall trends, demonstrating that stratospheric O_3 was not a likely cause for observed increases in western U.S. O_3.

In our HYSPLIT cluster analysis, we identified positive trends in median O_3 only within Clusters 2, 3, and 5, demonstrating that increasing springtime O_3 at MBO was most associated with rapid, high-altitude, trans-Pacific transport. These transport patterns together with reported trends in O_3 precursor emissions in East Asia support the hypothesis that increasing East Asian emissions and trans-Pacific transport have likely influenced western U.S. free tropospheric O_3 over the past decade.

4.2. CO

To verify and better understand the negative CO trend at MBO, we examined NOAA surface flask measurements at SHM, MID, and MLO (Figs. 3 and 4). All three sites showed significant negative trends in mean springtime CO from 2004 to 2012 (−2.8 ± 1.8 ppbv yr^{-1} (SHM); −2.6 ± 1.8 ppbv yr^{-1} (MID); −2.9 ± 2.6 ppbv yr^{-1} (MLO)). These trends, ranging from −2.4 to −1.7% yr^{-1}, are remarkably similar to the mean CO trend at MBO from 2004 to 2013 (−3.2 ± 2.9 ppbv yr^{-1}; −1.9% yr^{-1}), suggesting that the decline also applies broadly to the North Pacific region. A negative trend in Northern Hemisphere CO was previously observed in surface flasks from 1991 to 2001 (−0.92 ± 0.15 ppb yr^{-1}), a trend which was larger (−1.5 ppb yr^{-1}) when excluding 1997–1998 measurements that were highly influenced by wildfire emissions, and the overall decline was attributed to anthropogenic emissions reductions (Novelli et al., 2003).

Observations from the Aqua-AIRS instrument showed that springtime CO mixing ratios at 618 hPa near MBO decreased

Please cite this article in press as: Gratz, L.E., et al., Causes of increasing ozone and decreasing carbon monoxide in springtime at the Mt. Bachelor Observatory from 2004 to 2013, Atmospheric Environment (2014), http://dx.doi.org/10.1016/j.atmosenv.2014.05.076

Table 2
Linear regression statistics for springtime CO within HYSPLIT Clusters 1–7. Trends for Cluster 8 were not computed because no trajectories were assigned to it in 2004, 2007, or 2010. Bold values indicate $p < 0.05$.

CO	Mean				Median				5th percentile				95th percentile			
Cluster #	m (ppbv/yr)	b (ppbv)	r^2	p	m (ppbv/yr)	b (ppbv)	r^2	p	m (ppbv/yr)	b (ppbv)	r^2	p	m (ppbv/yr)	b (ppbv)	r^2	p
1	**−4.4**	**176**	**0.61**	**0.01**	**−5.4**	**182**	**0.66**	**0.00**	**−3.3**	**145**	**0.44**	**0.04**	−2.9	189	0.30	0.10
2	−3.4	172	0.31	0.09	−3.6	173	0.33	0.08	−2.3	136	0.20	0.20	−4.0	199	0.20	0.19
3	**−3.6**	**172**	**0.43**	**0.04**	**−3.9**	**174**	**0.47**	**0.03**	−2.4	135	0.16	0.25	−6.5	217	0.34	0.08
4	−3.7	163	0.39	0.05	−3.6	163	0.39	0.05	−4.5	139	0.34	0.08	−2.8	183	0.21	0.18
5	−2.9	162	0.36	0.07	**−2.8**	**162**	**0.43**	**0.04**	−3.4	130	0.32	0.09	−2.8	191	0.18	0.23
6	**−2.9**	**163**	**0.49**	**0.02**	**−2.4**	**158**	**0.45**	**0.03**	**−3.0**	**141**	**0.57**	**0.01**	−3.7	191	0.37	0.06
7	−2.6	148	0.25	0.14	−2.2	144	0.17	0.24	−2.9	126	0.19	0.21	N/A	N/A	N/A	N/A

by -2.1 ± 1.2 ppbv yr^{-1} from 2004 to 2012, while total column CO decreased by $-1.1 \pm 0.7\%$ yr^{-1}. Worden et al. (2013) similarly reported negative trends in Northern Hemisphere CO using daytime satellite column measurements for all seasons from thermal-infrared channels (sensitivity in middle to lower troposphere) with seasonal variations removed by a 12-month running average. For 8-year (12/2003–11/2011) and 11-year (12/2000–11/2011) periods, MOPITT satellite observations suggested significant declines in column CO of $-1.23 \pm 0.73\%$ yr^{-1} and $-0.92 \pm 0.51\%$ yr^{-1}, respectively (Worden et al., 2013). Springtime CO trends at MBO and the surface flask sites appear slightly larger than the satellite observations; however, they are comparable within reported uncertainties. Worden et al. (2013) also reported negative trends over eastern China of -1.0% yr^{-1} from 12/2003 to 11/2011 using AIRS retrievals and -1.6% yr^{-1} from 12/2000 to 11/2011 using MOPITT retrievals; however, given the low sensitivity of these retrievals to surface concentrations, the reported trends may not reflect trends in Asian CO emissions.

Global anthropogenic CO emissions decreased slightly from 1990 until 2000–2005, although there is large variability among different inventories and across regions (Granier et al., 2011). From 2000 to 2010, U.S. and European CO emissions declined by approximately -3% yr^{-1} while emissions in China and India increased by approximately 1.5% yr^{-1} and 3% yr^{-1}, respectively (Worden et al., 2013). However, Tohjima et al. (2013) recently suggested that these bottom-up CO emissions inventories underestimate total CO emissions from China by approximately 40% in part because they consider only primary CO emissions, while top-down estimates also reflect secondary CO production from non-methane VOC oxidation (Tohjima et al., 2013). Tohjima et al. (2013) estimated that total CO output (primary emissions and secondary oxidation products) from China increased from 1998/1999 to 2004/2005, then decreased after 2008/2009. The stabilization and recent decline may be related to improved combustion efficiency from pollution reduction measures implemented for the 2008 Olympic Games (Tohjima et al., 2013). Using annual emissions estimates from 2003/2004 to 2009/2010 (Table 1 in Tohjima et al. (2013)), a linear regression suggests Chinese CO emissions declined by -2.3% yr^{-1} ($r^2 = 0.56$, $p = 0.05$).

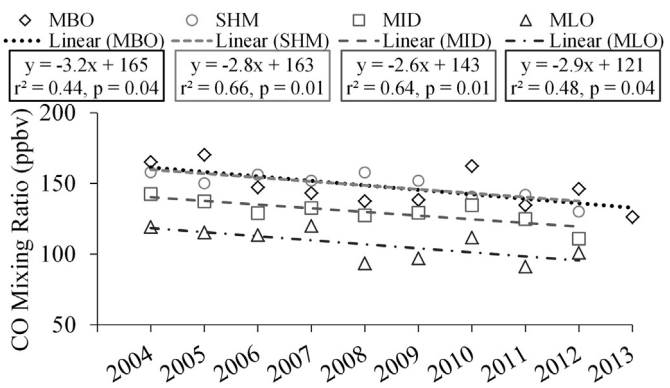

Fig. 4. Springtime mean CO mixing ratios at MBO for 2004–2013, and at NOAA surface flask sites for 2004–2012, with associated linear regressions.

If we take the analysis of Tohjima et al. (2013) to be more representative of Chinese CO emissions, these recent declines combined with reductions in European and North American emissions could partially explain the negative CO trend at MBO. HYSPLIT cluster analysis showed that decreasing CO at MBO was most associated with transport over the North Pacific and Siberia (Clusters 1 and 6). However, negative trends in median CO within Clusters 3 and 5 suggest that springtime CO associated with transport from East Asia may also be decreasing. These results point to a combination of decreasing emissions from North America and Europe broadly influencing CO in the northern mid-latitudes, as well as recent declines in total CO output from China affecting springtime CO at MBO.

We note that the median, 5th and 95th percentile CO in 2010 and the 95th percentiles in 2005 and 2012 were elevated relative to linear trends (Fig. 2). During spring 2010 exceptional Asian dust events associated with stable trans-Pacific transport strongly impacted western North America (Uno et al., 2011) and likely influenced CO mixing ratios at MBO. Springtime CO at MBO is also influenced by episodic boreal biomass burning. Increased biomass burning in spring or during summer/fall of the previous year can cause perturbations in CO relative to the long-term mean (Novelli et al., 2003). Intense biomass burning in Southeast Asia from winter 2004 through spring 2005 resulted in enhanced CO at MBO during April 2005 (Reidmiller et al., 2009a). Daily dry matter consumption (Tg/day) data from the Global Fire Assimilation System (Andela et al., 2013) suggests that biomass burning in Northern Asia was also moderately enhanced in spring 2012, which may have similarly influenced the 95th percentile CO at MBO.

We also acknowledge the complex relationship between O_3 precursor and CO emissions and the chemistry that occurs during atmospheric transport. For example, OH is the primary sink for CO, CH_4, and VOCs, while it is also a secondary product of O_3 photolysis (Novelli et al., 2003; Parrish et al., 2012). It is plausible that with increasing O_3 precursor emissions in Asia, atmospheric O_3 in the western U.S. would increase, while higher O_3 could lead to more OH production and consequently lower CO. Using the median springtime O_3 and CO trends at MBO, we approximate the net effect on North Pacific OH. We first assume that CO is the primary sink for OH. We then consider that O_3 photolysis produces O^1d, which reacts with H_2O to produce 2OH. We estimate the change in OH to be a factor of two multiplied by the change in O_3 divided by the change in CO. This amounts to a ~40% increase in North Pacific springtime OH over the 10-year period. If we assume CH_4 to be an equally important sink for OH, then the result is a ~20% increase in springtime OH. This simplified estimate does not consider other OH

Please cite this article in press as: Gratz, L.E., et al., Causes of increasing ozone and decreasing carbon monoxide in springtime at the Mt. Bachelor Observatory from 2004 to 2013, Atmospheric Environment (2014), http://dx.doi.org/10.1016/j.atmosenv.2014.05.076

sinks (e.g. NO_2, other hydrocarbons), but given the known reaction rates for OH with CO and CH_4, and considering our understanding of the composition of the remote North Pacific atmosphere, this may be a reasonable approximation.

5. Conclusions

We presented 10 years of springtime O_3 and CO measurements at MBO and identified the long-term trends. From 2004 to 2013, springtime median O_3 significantly increased while median CO significantly decreased. Analysis of the transport patterns associated with these trends suggests a dominant influence of ALRT on increasing springtime O_3. Decreasing springtime CO appears most associated with transport from the North Pacific where atmospheric CO is likely influenced by reductions in North American and European CO emissions. Additional declines were associated with East Asian transport that may be related to recent reductions in total CO output from China. The trends are consistent with others in the literature and suggest that East Asian emissions likely impact springtime western U.S. air quality. Future reductions in anthropogenic emissions in East Asia may therefore influence springtime surface O_3 in the western U.S., while domestic emissions reductions remain critical for reducing O_3 across the U.S. (Reidmiller et al., 2009b; Dentener et al., 2010). Continued long-term monitoring at sites like MBO will allow for further investigating the impact of domestic and intercontinental emissions and atmospheric transport on seasonal variability in O_3, CO, and other pollutants.

Acknowledgments

The National Science Foundation provided funding for measurements at MBO (grant AGS-1066032). We acknowledge NOAA ESRL-GMD for providing CO surface flask data and for support from Arlyn Andrews and Jonathan Kofler in CO measurements at MBO since 2012.

Appendix A. Supplementary data

Supplementary data related to this article can be found at http://dx.doi.org/10.1016/j.atmosenv.2014.05.076.

References

Ambrose, J.L., Reidmiller, D.R., Jaffe, D.A., 2011. Causes of high O_3 in the lower free troposphere over the Pacific Northwest as observed at the Mt. Bachelor Observatory. Atmos. Environ. 45, 5302–5315.

Andela, N., et al., 2013. Assessment of the Global Fire Assimilation System (GFASv1). Monitoring Atmospheric Composition & Climate – II. Path: http://atmosphere.copernicus.eu/about/project_structure/input_data/d_fire/.

Chen, H., et al., 2013. Accurate measurements of carbon monoxide in humid air using the cavity ring-down spectroscopy (CRDS) technique. Atmos. Meas. Tech. 6, 1031–1040.

Cooper, O.R., Ziemke, J., 2013. [Global climate] tropospheric ozone [in "state of the climate in 2012"]. Bull. Am. Meteorol. Soc. 94 (8), S38–S39.

Cooper, O.R., et al., 2010. Increasing springtime ozone mixing ratios in the free troposphere over western North America. Nature 463, 344–348.

Cooper, O.R., Gao, R., Tarasick, D., Leblanc, T., Sweeny, C., 2012. Long-term ozone trends at rural ozone monitoring sites across the United States, 1990–2010. J. Geophys. Res. 117, D22307.

Dentener, F., Keating, T., Akimoto, H. (Eds.), 2010. Hemispheric Transport of Air Pollution 2010: Part A: Ozone and Particulate Matter. Air Pollution Studies No. 17, U.N., New York and Geneva.

Draxler, R.R., Hess, G.D., 1998. An overview of the HYSPLIT_4 modeling system of trajectories, dispersion, and deposition. Aust. Meteorol. Mag. 47, 295–308.

Fischer, E.V., Jaffe, D.A., Weatherhead, E.C., 2011. Free tropospheric peroxyacetyl nitrate (PAN) and ozone at Mount Bachelor: potential causes of variability and timescale for trend detection. Atmos. Chem. Phys. 11, 5642–5654.

Forster, C., et al., 2004. Lagrangian transport model forecasts and a transport climatology for the Intercontinental Transport and Chemical Transformation 2002 (ITCT 2K2) measurement campaign. J. Geophys. Res. 109, D07S92.

Granier, C., et al., 2011. Evolution of anthropogenic and biomass burning emissions of air pollutants at global and regional scales during the 1980–2010 period. Clim. Change 109, 163–190.

Hartman, D.L., et al., 2013. Observations: atmosphere and surface. In: Stocker, T.F., et al. (Eds.), Climate Change 2013: the Physical Science Basis, Contribution of Working Group I to the 5th Assessment Report of the IPCC. Cambridge University Press, Cambridge, United Kingdom and New York, NY, USA.

He, H., et al., 2013. Trends in emissions and concentrations of air pollutants in the lower troposphere in the Baltimore/Washington airshed from 1997 to 2011. Atmos. Chem. Phys. 13, 7859–7874.

Jaeglé, L., Jaffe, D.A., Price, H.U., Weiss-Penzias, P., Palmer, P.I., Evans, M.J., Jacob, D.J., Bey, I., 2003. Sources and budgets for CO and O_3 in the northeastern Pacific during the spring of 2001: results from the PHOBEA-II Experiment. J. Geophys. Res. 108 (D20), 8802.

Jaffe, D., 2011. Relationship between surface and free tropospheric ozone in the western U.S. Environ. Sci. Technol. 45, 432–438.

Jaffe, D., Ray, J., 2007. Increase in surface ozone at rural sites in the western U.S. Atmos. Environ. 41, 5452–5463.

Jaffe, D., McKendry, I., Anderson, T., Price, H., 2003. Six 'new' episodes of trans-Pacific transport of air pollutants. Atmos. Environ. 37, 391–404.

Kahl, J.D., Samson, P.J., 1986. Uncertainty in trajectory calculations due to low resolution meteorological data. J. Clim. Appl. Meteorol. 25, 1816–1831.

Langford, A.O., Aikin, K.C., Eubank, C.S., Williams, E.J., 2009. Stratospheric contribution to high surface ozone in Colorado during spring. Geophys. Res. Lett. 36, L12801.

Lee, H.-J., et al., 2014. Transport of NO_x in East Asia identified by satellite and in situ measurements and Lagrangian particle dispersion model simulations. J. Geophys. Res. Atmos. 119, 2574–2596.

Lefohn, A.S., Wernli, H., Shadwick, D., Limbach, S., Oltmans, S.J., Shapiro, M., 2011. The importance of stratospheric-tropospheric transport in affecting surface ozone concentrations in the Western and Northern Tier of the United States,. Atmos. Environ. 45, 4845–4857.

Liang, Q., Jaeglé, L., Jaffe, D.A., Weiss-Penzias, P., Heckman, A., Snow, J.A., 2004. Long-range transport of Asian pollution to the northeast Pacific: seasonal variations and transport pathways of carbon monoxide. J. Geophys. Res. 109, D23S07.

Lin, M., et al., 2012a. Springtime high surface ozone events over the western United States: quantifying the role of stratospheric intrusions. J. Geophys. Res. 117 (D00V22).

Lin, M., et al., 2012b. Transport of Asian ozone pollution into surface air over the western U.S. in spring. J. Geophys. Res. 117 (D00V07).

Lin, M., Horowitz, L.W., Oltmans, S.J., Fiore, A.M., Fan, S., 2014. Tropospheric ozone trends at Mauna Loa Observatory tied to decadal climate variability. Nat. Geosci. 7, 136–143.

McDonald-Buller, E.C., et al., 2011. Establishing policy relevant background (PRB) ozone concentrations in the United States. Environ. Sci. Technol. 45 (22), 9484–9497.

Mijling, B., van der A, R.J., Zhang, Q., 2013. Regional nitrogen oxides emission trends in East Asia observed from space. Atmos. Chem. Phys. 13, 12003–12012.

Monks, P.S., et al., 2009. Atmospheric composition change – global and regional air quality. Atmos. Environ. 43, 5268–5350.

Moody, J.L., Munger, J.W., Goldstein, A.H., Jacob, D.J., Wofsy, S.C., 1998. Harvard Forest regional-scale air mass composition by Patterns in Atmospheric Transport History (PATH). J. Geophys. Res. 130 (D11), 13,181–13,194.

Novelli, P.C., Masarie, K.A., 2013. Atmospheric Carbon Monoxide Dry Air Mole Fractions from the NOAA ESRL Carbon Cycle. Cooperative Global Air Sampling Network, 1988-2012, Version: 2013-06-18, Path: ftp://aftp.cmdl.noaa.gov/data/trace_gases/co/flask/surface/.

Novelli, P.C., Masarie, K.A., Lang, P.M., Hall, B.M., Myers, R.C., Elkins, J.W., 2003. Reanalysis of tropospheric CO trends: effects of the 1997–1998 wildfires. J. Geophys. Res. 108 (D15), 4464.

Oltmans, S.J., et al., 2013. Recent tropospheric ozone changes – a pattern dominated by slow or no growth. Atmos. Environ. 67, 331–351.

Parrish, D.D., Aikin, K.C., Oltmans, S.J., Johnson, B.J., Ives, M., Sweeny, C., 2010. Impact of transported background ozone inflow on summertime air quality in a California ozone exceedance area. Atmos. Chem. Phys. 10 (20), 10093–10109.

Parrish, D.D., et al., 2012. Long-term changes in lower tropospheric baseline ozone concentration at northern mid-latitudes. Atmos. Chem. Phys. 12, 11485–11504.

Parrish, D.D., et al., 2013. Lower tropospheric ozone at northern midlatitudes: changing seasonal cycle. Geophys. Res. Lett. 40, 1631–1636.

Price, H.U., Jaffe, D.A., Cooper, O.R., Doskey, P.V., 2004. Photochemistry, ozone production, and dilution during long-range transport episode from Eurasia to the northwest United States. J. Geophys. Res. 109, D23S13.

Reidmiller, D.R., Jaffe, D.A., Chand, D., Strode, S., Swartzendruber, P., Wolfe, G.M., Thornton, J.A., 2009a. Interannual variability of long-range transport as seen at the Mt. Bachelor Observatory. Atmos. Chem. Phys. 9, 557–572.

Reidmiller, D.R., et al., 2009b. The influence of foreign vs. North American emissions on surface O_3 in the US. Atmos. Chem. Phys. 9, 5027–5042.

Rieder, H.E., Fiore, A.M., Polvani, L.M., Lamarque, J.-F., Fang, Y., 2013. Changes in the frequency and return level of high ozone pollution events over the eastern United States following emission controls. Environ. Res. Lett. 8, 014012.

Stohl, A., Eckhardt, S., Forster, C., James, P., Spichtinger, N., 2002. On the pathways and timescales of intercontinental air pollution transport. J. Geophys. Res. 107 (D23), 4684.

Strode, S.A., Pawson, S., 2013. Detection of carbon monoxide trends in the presence of interannual variability. J. Geophys. Res. Atmos. 118 http://dx.doi.org/10.1002/2013JD020258.

Tohjima, Y., et al., 2013. Temporal changes in the emissions of CH_4 and CO from China estimated from CH_4/CO_2 and CO/CO_2 correlations observed at Hateruma Island. Atmos. Chem. Phys. Discuss. 13, 22893–22930.

Uno, I., et al., 2011. Large Asian dust layers continuously reached North America in April 2010. Atmos. Chem. Phys. 11, 7333–7341.

U.S. Environmental Protection Agency (EPA), 2010. National ambient air quality standards for ozone, proposed rules. Fed. Regist. 75 (11), 2938–3052.

Weiss-Penzias, P., Jaffe, D.A., Swartzendruber, P., Dennison, J.B., Chand, D., Hafner, W., Prestbo, E., 2006. Observations of Asian air pollution in the free troposphere at Mount Bachelor Observatory during the spring of 2004. J. Geophys. Res. 111, D10304.

Wigder, N., Jaffe, D.A., Herron-Thorpe, F.L., Vaughn, J.K., 2013a. Influence of daily variations in baseline ozone on urban air quality in the United States Pacific Northwest. J. Geophys. Res. 118, 3343–3354.

Wigder, N., Jaffe, D.A., Saketa, F.A., 2013b. Ozone and particulate matter enhancements from regional wildfires observed at Mount Bachelor during 2004–2011. Atmos. Environ. 75, 24–31.

Worden, H.M., et al., 2013. Decadal record of satellite carbon monoxide observations. Atmos. Chem. Phys. 13, 837–850.

Zhang, L., et al., 2008. Transpacific transport of ozone pollution and the effect of recent Asian emission increases on air quality in North America: an integrated analysis using satellite, aircraft, ozonesonde, and surface observations. Atmos. Chem. Phys. 8, 6117–6136.

Zhao, B., et al., 2013. NO_x emissions in China: historical trends and future perspectives. Atmos. Chem. Phys. 13, 9869–9897.

Please cite this article in press as: Gratz, L.E., et al., Causes of increasing ozone and decreasing carbon monoxide in springtime at the Mt. Bachelor Observatory from 2004 to 2013, Atmospheric Environment (2014), http://dx.doi.org/10.1016/j.atmosenv.2014.05.076